

On-site holographic interference method for fast surface topology measurements and reconstruction

This content has been downloaded from IOPscience. Please scroll down to see the full text.

2015 Phys. Scr. 90 065502

(<http://iopscience.iop.org/1402-4896/90/6/065502>)

View [the table of contents for this issue](#), or go to the [journal homepage](#) for more

Download details:

IP Address: 194.102.58.6

This content was downloaded on 19/06/2015 at 06:20

Please note that [terms and conditions apply](#).

On-site holographic interference method for fast surface topology measurements and reconstruction

L Ionel¹, D Ursescu^{1,2}, L Neagu^{1,2} and M Zamfirescu¹

¹National Institute for Laser, Plasma and Radiation Physics, Laser Department, Atomistilor 409, PO Box MG-36, 077125, Măgurele-Bucharest, Romania

²Extreme Light Infrastructure Nuclear Physics (ELI-NP)/Horia Hulubei National Institute for R and D in Physics and Nuclear Engineering (IFIN-HH), 30 Reactorului St., Bucharest-Magurele, jud. Ilfov, POB MG-6, RO-077125, Romania

E-mail: laura.emilia.ionel@gmail.com

Received 24 November 2014, revised 17 March 2015

Accepted for publication 13 April 2015

Published 1 May 2015



CrossMark

Abstract

Based on holographic interferometry technique, we develop a quantitative method for on-site characterization of surface topology and 3D reconstruction. The optical set-up with 2D spatial light modulator for surface characterization of 3D micro-structures is presented. It is shown that this non-destructive and non-contact method made possible the rapid investigation of 3D polymer structures employing diffractive masks and phase modulation based on two beams interference. The experimental results obtained with this method demonstrated the quantitative high-resolution measurement of samples topology with faster processing details comparing to the actual screening methods which cannot be used on-site conditions.

Keywords: spatial light modulators, surface reconstruction, holographic interferometry, topologic measurements

(Some figures may appear in colour only in the online journal)

1. Introduction

For surface topology characterization, typically used technologies are atomic force microscopy, scanning electron microscopy, interferometric microscopy, white light interferometry (WLI). Each method is applied on specific application, requiring high resolution or large area of measurement. Lately, due to the actual needs in terms of reducing the time of the surface imaging, faster characterization methods were developed. However, none of the above methods can provide a fast and on-site measurement of the surface characteristics. As an example, high laser power facilities requires methods to characterize the optical components on-site, avoiding the un-mounting or replacement of the big optical parts.

Digital holographic imaging, combined with classical holography and post-digital image processing technique started to be implemented as a new fast technology in a wide range of applications concerning the surface topography

measurements of micro-structure objects [1]. Digital holographic measurement, in association with adaptive optical devices (e.g. liquid crystal spatial light modulators (SLMs)) is able to retrieve the surface topology of microstructures using a non-contact and non-invasive method offering a fast and high precision characterization [2].

Liquid crystal SLMs have been demonstrated lately as the most efficient configurable opto-electronic element to compensate the aberrations of optical fields. These devices are able to modulate light spatially in amplitude and/or phase and the optical information to be displayed can be taken directly from the dedicated software or an image source and can be addressed by a computer interface. In recent decades, SLMs were successfully implemented in many applications such as: wave front correction [3, 4], compensating time-varying aberration of optical fields [5], compensation of thermal phase distortion occurring in high-energy Nd:glass amplifiers [6], beam steering [7], holographic optical tweezers [8], multi-focal multiphoton microscopy [9], edge contrast improvement

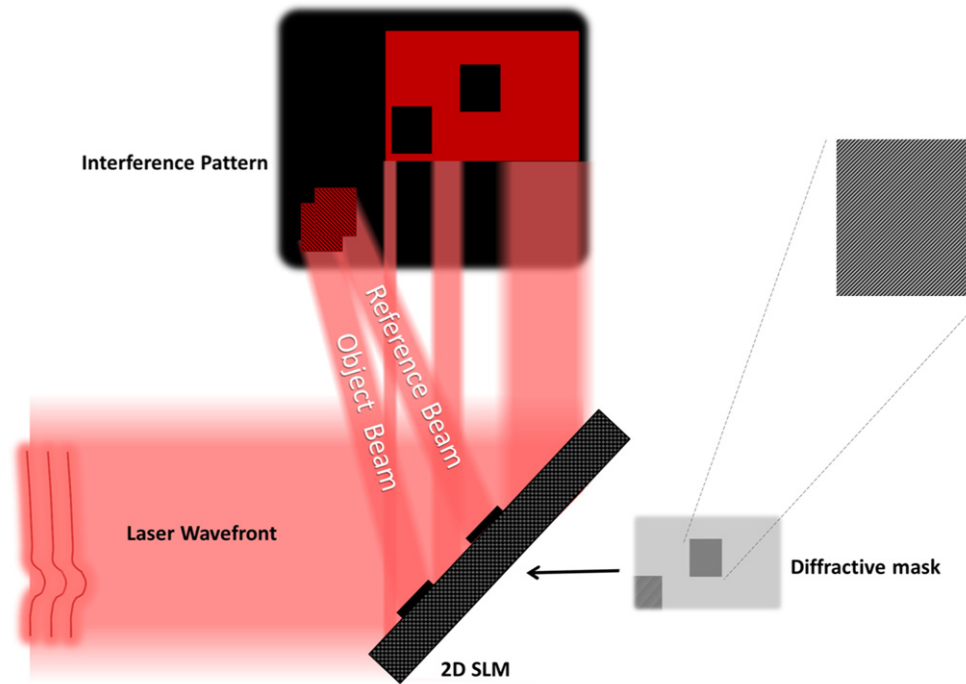


Figure 1. Projecting optical pattern reconstruction setup with two blazed diffraction gratings mask.

in light microscopy [10], holographic data storage [11], image processing and analysis [12], beam-quality measurements [13]. Also, they can act like programmable phase masks [14, 15], diffractive microlenses [16], multiple beam splitters [17], optical switches [18] or beam shapers [19].

In this paper we built an experimental setup for investigation and reconstruction of the three-dimensional surface topology of polymer microspheres. The characterization method is based on measurements of interference fringes of two beams generated by an SLM using diffractive masks. To this purpose, the SLM has been used both as a beam splitter for the object and the reference beam at the same time and as a beam steering device which performs a precise control in a wide range on the angle between the beams which interfere on the CCD camera. This method was design to offer high resolution and fast non-destructive characterization of the surface topology of microstructures. Also, the proposed method proves to be adequate for samples that have a region where the structures are absent.

2. Theoretical approach: diffraction masks generation for SLM

An innovative optical measurement method of surface microstructures was developed. The characterization of the surface topology is based on the direct and on-site comparison of the micro-patterned area with the remaining non-structured part of the same object.

According to the basic principle of holography two beams, the reference beam and the object beam are computer generated using an SLM. A diffractive mask is converted to phase image on the SLM. The masks displayed on the SLM

consist of two blazed diffraction gratings with slightly different line spacing and grooves orientation relative to the incident beam. The reference beam corresponds to the non-structured area of the sample, while the object beam carries out the phase information of the surface microstructures. The two laser spots interfere out of the beam directly reflected by the SLM. In the image plane, we obtain a two overlapped images pattern which contains the information of the surface topology of interest to be decrypted (figure 1). These tasks are realized by simple changing of the gratings parameters addressed on the both zones of SLM display, which gives a good scalability and control for the method.

The phase gratings orientation controls the two laser beams propagation plane, while the different line spacing of them controls the beams direction in the propagation plane.

Initially, a complex study for different angles between the rays which interfere on the CCD detector has been performed in order to establish the proper value of the interfringe distance in the image plane and to achieve a good overlapping of the two laser beam spots. This angle value is given by the position of the two gratings on the diffraction mask. The distance between the two gratings was calculated in accordance with the two parameters of the gratings and the distance between the SLM and the image plane in order to obtain the two overlapped images pattern in a well-defined zone, out of the zero-order diffraction.

Once the desired parameters are established a grayscale mask is computed and afterward electronically addressed to the SLM. Each gray level of the mask introduces a different value of the electronically addressable potential on the SLM pixels and consequently different refractive index and phase shift in the optical path of the incident beam. During the images acquisition the masks configuration remains unchanged.

When two laser beams are superimposed in order to interfere, the resulting overall intensity recorded by the CCD camera can be expressed as:

$$I_{\text{tot}} = I_1 + I_2 + 2I_1I_2 \cos(\phi_1 - \phi_2), \quad (1)$$

where I_1 , I_2 , ϕ_1 and ϕ_2 represents the intensity and the phase, respectively, of each of the two overlapped beams.

From the interference pattern generated by the two laser beam the maximum values of the interference fringes are recorded and processed in order to extract the linear phase gradient. The quantitative phase distribution of the beam coming from the sample is calculated from the imparted gradient field following [2].

The numerical algorithm that we elaborated adopts the 8-bit type interference images registered by the CCD camera.

The overall intensity of the interference patterns depends on the phase difference ($\Delta\Phi$) between the two overlapped laser beams of wavelength λ and this can be written as:

$$\Delta\phi = \phi_1 - \phi_2 = \frac{2\pi L_{1,2}(\sin\theta_1 - \sin\theta_2)}{\lambda}. \quad (2)$$

Here L is the fringe spacing and θ_1 and θ_2 are given by the phase grating orientation. Therefore the relation (2) becomes:

$$\Delta\phi = \frac{2\pi}{\lambda} \cdot d_{x,y}, \quad (3)$$

where $d_{x,y}$ is the optical path difference between the beams, considered for each (x, y) point in the beam profiles in the image plane. Here the highest intensities correspond to the zero phase differences and the lower intensities are recorded when the beams are in opposite phases.

The goal of this method is to extract the phase difference from the position of the maximum intensities of the fringes and to determine numerically the optical path difference in order to retrieve the sample surface topology. The numerically reconstruction method is described in section 4.

The image plane position is imposed by the superposition of the two laser beams.

3. Experimental setup

The test sample is a commercial glass plate. The glass plate area is 2 cm^2 with smooth surface and planarity better than $\lambda/4$. In our work a two-row array of SU8 polymer micro-spheres were imprinted on half from the test sample area using a conventional polymerization method, in order to test the capability of our method to characterize the surface profile. The non-structured part of the sample was used as reference.

The light source used for interferometric characterization of the samples is a He-Ne laser with emission spectrum centered at 632.8 nm. A $5\times$ telescope was used to enlarge the laser spot diameter and to uniformly illuminate the all active area of the SLM.

The SLM is a PLUTO model from HOLOEYE with liquid crystal-on-silicon (LCOS) active matrix reflective phase only sensor. The active area has $15.36 \times 8.64 \text{ mm}$ size, with a VGA graphic card resolution (1920 columns and 1080

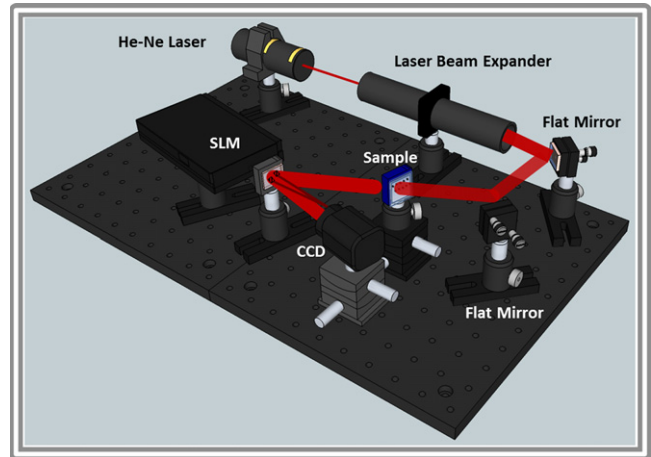


Figure 2. Schematic representation of the setup based on a 2D LCOS SLM for optical micro-structured surface characterization.

rows active pixels), $8 \mu\text{m}$ pitch, 60 Hz image frame rate, phase-only modulation. The final images are recorded on the CCD (Point-Gray GS3-U3-60S6M-C) with the pixel pitch of $4.5 \mu\text{m}$, sufficient to record diffraction limited images on a high resolution.

In figure 2 the schematic of the optical set-up is presented. The expanded laser beam uniformly irradiates the sample area. The specimen is mounted on a XY translation stage, able to be displaced with high accuracy with μm range steps in order to achieve a full scanning of the surface. The wave front of the reflected beam is modulated according to the sample surface topology, and then propagates to the SLM. We addressed on the SLM the diffractive masks computer generated in order to obtain the interference image in the CCD image plane. For each XY displacement, the interference images are recorded and processed in order to obtain the phase gradient.

4. Results and discussions

The method described here generates interference images using diffractive masks which create the two beams to be overlapped, the reference beam and the object beam corresponding to the non-structured and respectively to the structured area of the test sample. The masks, displayed as gray scale images on the computer screen, are converted to phase images on the SLM. The masks on SLM were generated with Mathematica code, taking into account the laser source wavelength. The calculated masks consist of two blazed diffraction gratings with periodicity of 50 cycles per 300 pixels with no phase difference between the gratings.

To demonstrate the quantitative capabilities of the proposed method, we have compared both test sample surface profiles, non-structured as reference, and micro-structured as specimen, using two methods, the standard WLI technique and our interferometric method.

First we have attempt to measure the topology of the surface of the micro-structured test specimen by WLI method. Figure 3 shows a schematic representation of the specimen to

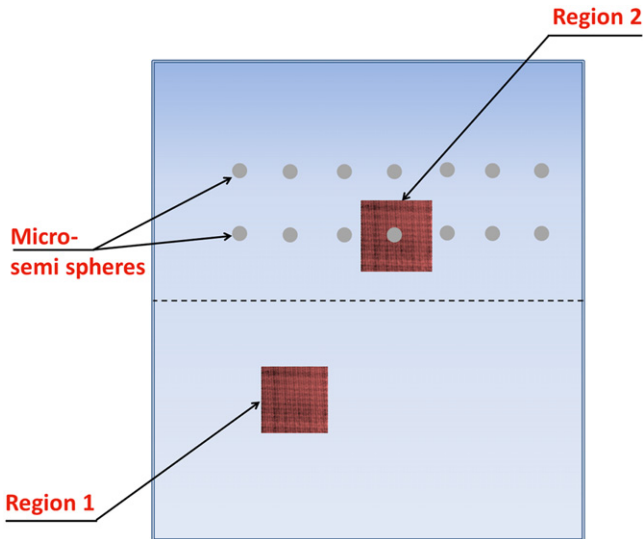


Figure 3. The sketch of the glass plates used as specimen indicating the two regions involved in the interferometric image retrieval method.

be analyzed indicating the two regions of the surface to be investigated: the reference area of the sample (Region 1), and the region of interest (Region 2), which corresponds to the reference beam and object beam, respectively. The maximum area which can be visualized at one surface investigation in actual conditions is limited by the SLM display dimensions, in order to create two separated zones on the SLM display. The surface flatness of the test specimen is considered to be within the limits imposed by the manufacturer so that the roughness spikes height does not exceed 10 nm.

The polymer micro-spheres were formed on half of the test sample surface. Thus, the second half surface of the specimen, which corresponds to the reference beam, does not present micro-structures. The distance between the micro-structures had been set to approximately $1500\ \mu\text{m}$. Thus, we ensure accurate results provided by a well defined interferometric pattern due to a rigorous separation of both reference and specimen areas. The minimum dimension which can be resolved depends on the SLM display resolution, CCD display resolution and the diffraction gratings parameters. Initially, several tests have been made in order to establish the working parameters and we found that this method in our experimental conditions can provide surface details of structures with dimensions down to $50\ \mu\text{m}$ and minimum height of around a few hundred nanometers.

The test specimen is shown by WLI image depicted in figure 4(a). The test specimen profile measured by WLI technique is illustrated in figure 4(b) and it offers the specific details related to the topology of the investigated micro-semisphere. The polymer micro-structure is found to have a diameter of $220\ \mu\text{m}$ and a height of $6.72\ \mu\text{m}$.

The WLI results have been compared with the interferometric measurements for the test sample. This method allows the experimental determination of the phase difference and hence, if we achieve the optical path difference from this gradient field, then we can obtain the final quantitative results.

The phase difference between the reference and object beams gives information related to the path difference $d_{x,y}$, necessary for the surface topology reconstruction. Related to (3), the optical path difference can be written as:

$$d_{x,y} = \frac{\Delta\phi \cdot \lambda}{2\pi}. \quad (4)$$

In order to reconstruct the specimen surface, a numerical code was built, which first converts the interference image in an array of pixels values.

Then, it identifies each maximum value of the fringes pattern pixels by reading the pixels line by line, as integers in the range of 0–255 in a matrix of pixels values.

Therefore, we established the position of each of them in the union-built matrix from which the phase difference between the two beams can be determined.

According to equation (4), the numerical algorithm can now calculate the optical path difference needed to generate the three-dimensional representation of the shape of the investigated sample area. This is possible by plotting the data matrix generated by the joint of the previously mentioned data matrices taking into account the shape details given by the optical path difference ($d_{m,n}$) on each pixel position ($\text{Pos}_{m,n}$):

$$M_{3D} = \begin{bmatrix} \{ \text{Pos}_{1,1}, P_{\max 1,1}, d_{1,1} \}, \\ \{ \text{Pos}_{1,2}, P_{\max 1,2}, d_{1,2} \}, \dots, \\ \{ \text{Pos}_{1,n}, P_{\max 1,n}, d_{1,n} \}, \\ \{ \text{Pos}_{2,1}, P_{\max 2,1}, d_{2,1} \}, \dots, \\ \{ \text{Pos}_{2,n}, P_{\max 2,n}, d_{2,n} \}, \dots, \\ \{ \text{Pos}_{m,n}, P_{\max m,n}, d_{m,n} \} \end{bmatrix}. \quad (7)$$

Figure 5 shows the test surface topology reconstructed by the numerical code which is based on the optical processing features previously described. By using an XYZ stage, the CCD camera is able to capture successive frames after a complete scanning of the sample at micrometer scale. The image that was analyzed by the numerical code has 300×300 pixels dimensions and it corresponds to the region investigated by WLI.

The specific topologic details had been quantified by using the numerical code applied on the corresponding interference pattern (figure 5(a)). Figure 5(b) shows a three-dimensional representation of the region of interest which was reconstructed following the numerical procedure previously described. An image profile through the center of the micro-sphere offers the details referring to the micro-structure shape (figure 5(c)). The investigated micro-sphere has a width of $220\ \mu\text{m}$ and a height of $6.8\ \mu\text{m}$. These results are in agreement with the WLI measurements of the surface specimen, proving in this way the efficiency of this interferometric method of surface image retrieval. The analysis presented above was repeated on the same test sample for a further several different regions to investigate the efficiency of the method. In all cases, the range of the maximum highness of the micro-spheres was in agreement with the WLI results.

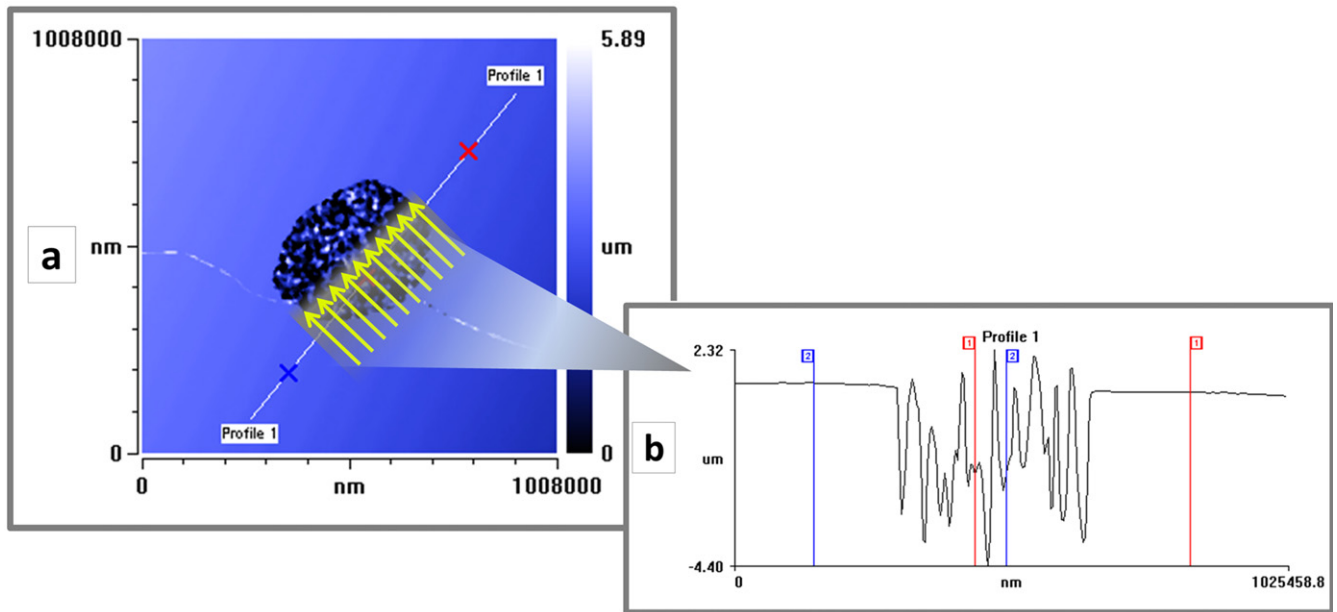


Figure 4. Polymer micro-structures specimen. (a) WLI image of the polymer micro-semi-sphere to be investigated; (b) WLI profile of the peak to valley measurement of the micro-semi-sphere.

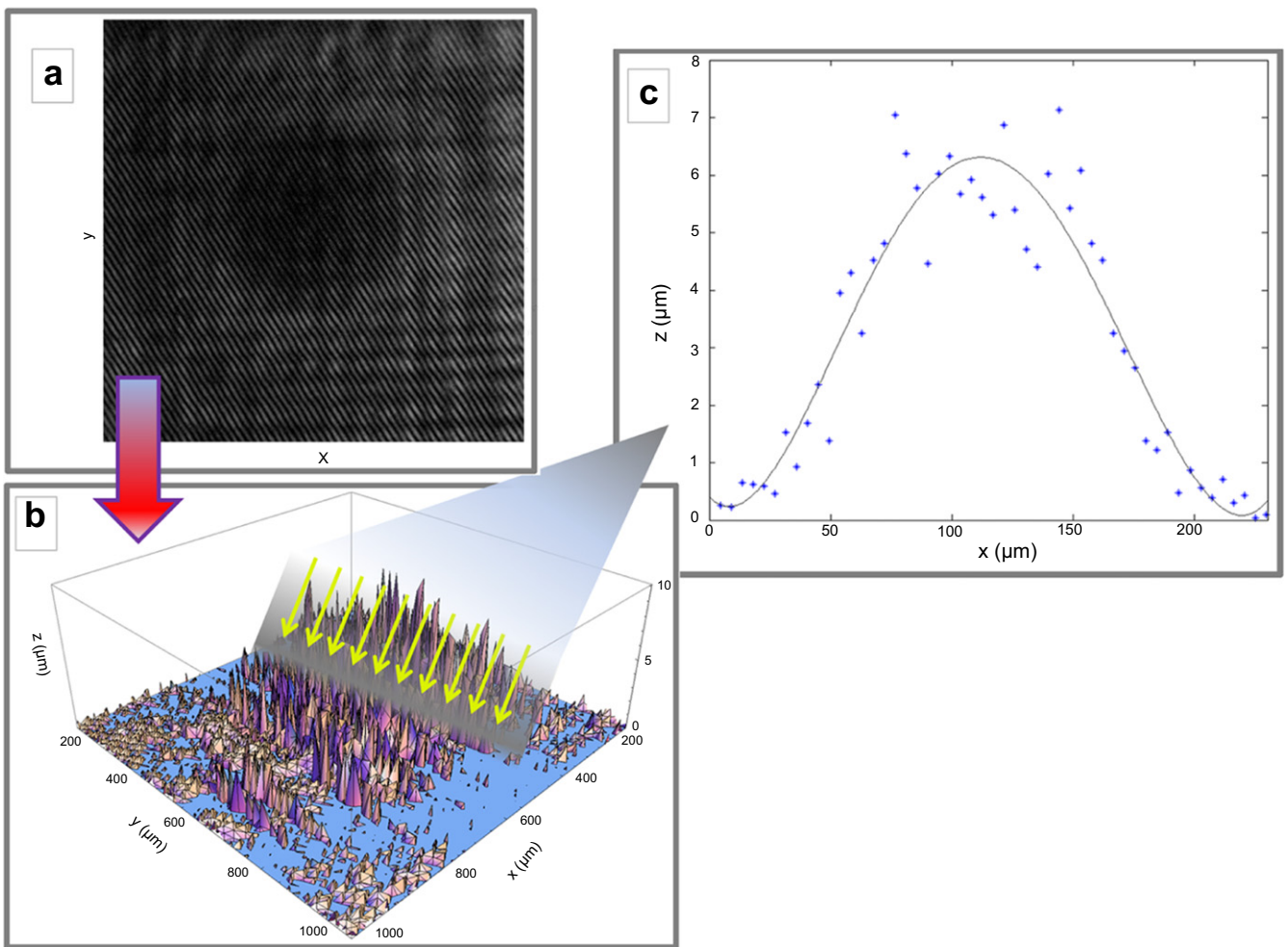


Figure 5. (a) The interference pattern from the region of interest with one test object recorded using an off-axis holographic setup; (b) numerical reconstruction of the test specimen surface by using the fringes interference method; (c) cross-section taken from top to bottom through the center of the polymer micro-semi-sphere.

5. Conclusions

An innovative on-site imaging measurement method of microstructures surface was developed based on two beams interference. This method was design to offer a fast non-destructive measurement of the surfaces topology. Using a XY stage or a rotation mount, the complete scanning for a defined surface is possible. Using the presented numerical algorithm, surface mapping can be rapidly done. The flexibility offered by the SLM allows to this surface reconstruction method to be fast and easy implementable and applicable for a wide range of samples with specific topology.

The technique was successfully used to measure the surface topology of micro-structures. The reconstructed images shown that the numerical code allows the retrieval of the surface features profile with good accuracy, in agreement with other profiling methods. The method presented here opens the perspectives of performing surface topology measurements using a SLM illuminated by a continuous laser source. This simple configuration of the setup offers the possibility to be easily implemented and can supports upgrades in order to increase the final images resolution and to improve the efficiency and accuracy of the surface topological measurements. The described technique could be further improved by the use of XY translation stages with larger travel range for scanning of full sample area which could extend the dimensions of the investigated area.

Acknowledgments

This work was supported by UEFISCDI, Project PN-II-ID-PCE-2012-4-0539, Contract No. 33/2013 and Project PN-II-PT-PCCA-2011-3.1-0886, Contract No. 1/2012

References

- [1] Mihailescu M, Scarlat M, Gheorghiu A, Costescu J, Kusko M, Paun I A and Scarlat E 2011 *Appl. Opt.* **50** 3589–97
- [2] McIntyre T J, Maurer C, Fassel S, Khan S, Bernet S and Ritsch-Marte M 2010 *Opt. Express* **18** 14063–78
- [3] Jesacher A, Schwaighofer A, Fürhapter S, Maurer C, Bernet S and Ritsch-Marte M 2007 *Opt. Express* **15** 5801–8
- [4] García-Márquez J, Landgrave J E A, Alcalá-Ochoa N and Pérez-Santos C 2011 *Opt. Lasers Eng.* **49** 743–8
- [5] Hardy J W 1998 *Adaptive Optics for Astronomical Telescopes* (New York: Oxford University Press)
- [6] Wattellier B, Chanteloup J C, Fuchs J, Sauteret C, Zou J P and Migus A 2001 *Conf. on Lasers and Electro-Optics, Technical Digest Series* (Washington, DC: Optical Society of America) pp 70–1
- [7] Xun X, Chang X and Cohn R W 2004 *Opt. Express* **12** 260–8
- [8] R Dufresne E and Grier D G 1998 *Rev. Sci. Instrum.* **69** 1974–7
- [9] Shao Y, Qin W, Liu H, Qu J, Peng X, Niu H and Gao B Z 2012 *Appl. Phys. B* **107** 653–7
- [10] Fürhapter S, Jesacher A, Bernet S and Ritsch-Marte M 2005 *Opt. Express* **13** 689–94
- [11] Das B, Joseph J and Singh K 2009 *Opt. Commun.* **282** 2147–54
- [12] Nagaev A I, Parygin V N and Pashin S I 1982 *Sov. J. Quantum Electron.* **12** 1178–81
- [13] Schulze C, Flamm D, Duparré M and Forbes A 2012 *Opt. Lett.* **37** 4687–9
- [14] Weiner A M 2000 *Rev. Sci. Instrum.* **71** 1929–61
- [15] Berberova N, Stoykova E and Sainov V 2012 *Phys. Scr.* **T149** 014020:01–014020:04
- [16] Mihailescu M, Preda A M, Sobetskii A and Petcu A C 2009 *Opto-Electron. Rev.* **17** 330–7
- [17] Moradi A, Ferrari E, Garbin V, Fabrizio E and Cojoc D 2007 *Optoelectron. Adv. Mater.- Rapid Commun.* **1** 158–61
- [18] Ahderom S, Raisi M, Lo K, Alameh K E and Mavaddat R 2002 *High speed networks and multimedia communications 5th IEEE Int. Conf.* pp 239–42
- [19] Mihailescu M 2010 *Opt. Express* **18** 12526–36